JOURNAL OF PROPULSION AND POWER
Vol. 16, No. 4, July–August 2000

Stability of Plane Liquid Sheets in Compressible Gas Streams

Jianming Cao*
Chang'an University, 710064 Xi'an, People's Republic of China
and
Xianguo Li†
University of Waterloo, Waterloo, Ontario N2L 3G1, Canada

A linear stability analysis has been carried out for viscous incompressible liquid sheets in two compressible gas streams of unequal velocities. It is found that there exist two independent unstable modes: parasinuous and paravaricose. Although both modes are unstable, the parasinuous mode is predominant under the conditions typically found for practical applications of liquid atomization and sprays. Gas compressibility increases the wave growth rate and dominant wave number for both of the unstable modes; hence, it can enhance significantly the breakup of liquid sheets and the production of small droplets in sprays.

Nomenclature

a = half-thickness of the liquid sheet
C = velocity of sound for the gas phase
d_j = gas-to-liquid density ratio, $\bar{\rho}_j/\bar{\rho}_\ell$
i = $\sqrt{-1}$
k = wave number
M_j = Mach number of the ambient gas with respect to a frame of reference moving with the liquid sheet at a velocity U_ℓ^*, U_ℓ^*/C_j
m = ka
p = pressure perturbation
Re = liquid Reynolds number, $U_\ell^* a/\nu_\ell$
r_j = $d_j[1 + (\Omega + imU_j)^2 M_j^2/m^2]^{-1/2}$
S = $[m^2 + Re(\Omega + im)]^{1/2}$
t = time
U_j = dimensionless gas stream velocity, U_j^*/U_ℓ^*
U_ℓ^* = liquid sheet velocity
U_1^*, U_2^* = gas stream velocity
u = x component of the velocity perturbation
$\boldsymbol{u}$ = velocity perturbation vector
v = y component of the velocity perturbation
We = liquid Weber number, $\rho_\ell U_\ell^{*2} a/\sigma$
x = spatial coordinate parallel to the liquid sheet and in the direction of flow
y = spatial coordinate normal to the liquid sheet
η = surface displacement from the unperturbed position $y = \pm a$
η_0 = initial disturbance amplitude
μ = dynamic viscosity
ν = kinematic viscosity
ρ = density perturbation
$\bar{\rho}$ = density
σ = surface tension
Ω = $\omega a/U_\ell^*$
ω = eigenfrequency

Subscripts

Im = imaginary part of a complex variable
j = ℓ, 1 or 2
ℓ = liquid-phase property
Re = real part of a complex variable
1 or 2 = property associated with the upper or lower gas stream, respectively
$+$ = upper gas–liquid interface
$-$ = lower gas–liquid interface

Received 10 December 1998; revision received 13 December 1999; accepted for publication 16 March 2000.

*Lecturer, Department of Automobile Engineering; currently Associate Professor, Faculty of Automobile Engineering; jmcao@pub.xaonline.com.
†Professor, Department of Mechanical Engineering; X6Li@uwaterloo.ca.

Introduction

THE instability and breakup of thin liquid sheets into small droplets are of significant fundamental and practical importance and have a variety of practical applications, such as spray drying operations, chemical and pharmaceutical processing, and power generation and propulsion systems.[1,2] As a result, a number of studies have been carried out to investigate various aspects of liquid sheet stability and breakup processes. A summary of the early studies can be found in Ref. 3 as they relate to the application of liquid atomization and sprays. Squire[4] and Hagerty and Shea[5] conducted a stability analysis of a thin liquid sheet with both liquid and gas phases being taken as inviscid and incompressible. Hagerty and Shea[5] showed that there can only exist two modes of unstable waves on the two gas–liquid interfaces for liquid sheets in a stationary gas medium, corresponding to the two surface waves oscillating exactly in and out of phase, commonly referred to as the sinuous and varicose modes. They also performed the first experimental measurements of the wave growth and wavelength for liquid sheets under various flow conditions, and the theoretical predicitions were compared favorably with their experimental results. The effect of liquid viscosity was investigated by Li and Tankin.[6] It was shown that although aerodynamic instability dominates and viscous effect reduces the wave growth rate for the sinuous mode at large Weber numbers and for the varicose mode at any Weber numbers, liquid viscosity can enhance the liquid sheet instability for the sinuous mode at low Weber numbers, and under this condition the viscosity-enhanced instability can even become predominant. Li[7] also carried out a study on the stability of viscous liquid sheets in two gas streams of unequal velocities. It was found that two independent unstable modes, named parasinuous and paravaricose, exist for this case, and that these modes resemble, but certainly differ from, the well-known sinuous and varicose modes found by Hagerty and Shea[5] for liquid sheets in a stationary gas medium. It was also shown that the relative velocities between the liquid and gas streams control the paravaricose mode and the parasinuous mode at large Weber numbers and that the absolute velocities of the liquid and gas streams dominate the parasinuous mode at small Weber numbers.

All of these previous studies have considered the liquid sheet instability as a result of temporally growing disturbances. Lin et al.[8] investigated the absolute and convective (spatial) instability of a liquid sheet. The spatial instability of plane liquid sheets was also studied by Li.[9] He showed that, for the practical importance of large Weber numbers for the application of liquid atomization and sprays,

the spatial instability is related to the temporal instability according to Gaster's transformation.[10] The various results concerning the absolute and spatial instability of plane liquid sheets have also been reviewed by Li.[11]

In all of the aforementioned theoretical studies, both liquid and gas phases have been assumed incompressible. However, it is well known that in practice the compressibility effect may not be neglected, such as in twin-fluid, for example, air assist and airblast, atomization, where the relative velocity between the gas and liquid sheet could reach as high as close to the sonic velocity of the gas, and in scramjet combustors, where liquid fuel jets are injected transversely into a supersonic flow of gas. Twin-fluid atomization is extensively used in many industrial processes, including fuel preparation in jet engines[2] and spray drying processes.[1] Hence, a theoretical study of the compressibility effect on liquid sheet instability becomes necessary. Li and Kelly[12] analyzed the stability of an inviscid incompressible liquid sheet and circular liquid jet in a coflowing compressible gas stream, and the effect of compressibility on circular liquid jet instability has also been studied for two- (Refs. 13–15) and three-dimensional disturbances.[16] However, the general case of the instability of viscous liquid sheets in two compressible gas streams of unequal velocities has not been investigated, and this is the subject of the present study.

Experimental observations of the liquid sheet disintegration in high-velocity coflowing gas streams[17,18] clearly indicate the existence of the two-dimensional unstable waves, especially in the early stage of the sheet breakup process. Theoretically, Squire's theorem (see Ref. 19) is applicable for the present case of linear stability of two-dimensional liquid sheets, so that for any unstable three-dimensional disturbances there exists an equivalent two-dimensional disturbance that is more unstable. Because the present study is interested in the instability and breakup of liquid sheets, only two-dimensional disturbances will be considered. The linear stability analysis will be presented next, leading to the dispersion relation governing the characteristics of the liquid sheet instability. Then the results will be given, followed by the conclusions drawn from the present investigation.

Stability Analysis

Consider a two-dimensional viscous liquid sheet with a thickness of $2a$, a velocity U_ℓ^*, and density $\bar{\rho}_\ell$ discharged into two compressible gas streams of unequal velocities, as shown schematically in Fig. 1. The gas stream on one side of the liquid sheet has a velocity U_1^* and density $\bar{\rho}_1$ and on the other side has a velocity U_2^* and density $\bar{\rho}_2$. Because of its inherent nature, the liquid sheet with the aforementioned flowfield is unstable subject to even small disturbances. Assume $\boldsymbol{u}_j = (u_j, v_j) = \boldsymbol{u}_j(x, y, t)$, $p_j = p_j(x, y, t)$, and $\rho_j = \rho_j(x, y, t)$ are the velocity, pressure, and density perturbations, respectively, induced by a disturbance. Then the equations governing these perturbation quantities are the conservation of mass and momentum, which can be written, on linearization, as follows:

$$\left(\frac{\partial}{\partial t} + U_j^*\frac{\partial}{\partial x}\right)\rho_j = -\bar{\rho}_j \nabla\cdot\boldsymbol{u}_j \tag{1}$$

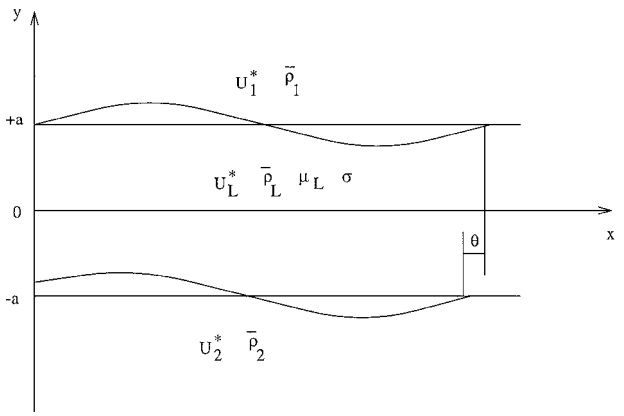

Fig. 1 Schematic of a plane liquid sheet.

$$\left(\frac{\partial}{\partial t} + U_j^*\frac{\partial}{\partial x}\right)\boldsymbol{u}_j = -\frac{1}{\bar{\rho}_j}\nabla p_j + \nu_j\nabla^2\boldsymbol{u}_j \tag{2}$$

where the subscript $j = \ell$ represents the quantities related to the liquid phase, and $j = 1$ or 2 to the gas phase on each side of the liquid sheet. Here it is assumed that the gravity is negligible, that the liquid phase is incompressible ($\bar{\rho}_\ell = 0$), and that the gas phase is inviscid, that is, that the gas kinematic viscosity $\nu_1 = \nu_2 = 0$. The effect of gravity has been neglected because the Froude number involved is typically very large for practical applications of liquid atomization and sprays. The liquid-phase compressibility effect has been shown to be negligible for cylindrical liquid jets[13,14] and is expected to be the same for the present problem. The neglect of gas viscosity is based on the observation that the viscosity of the surrounding gas medium is only weakly stabilizing and does not influence the relevant phenomenon appreciably, as Lin and Ibrahim[20] found in a related work. It has also been shown[21] that the shear waves at the liquid–gas interface due to the growth of boundary layers play a secondary role in the jet breakup process (the effect is orders of magnitude smaller than those considered herein).

Because the gas phase is compressible, one more equation is needed to specify the gas motion, which is the equation of state:

$$\left(\frac{\partial p_j}{\partial \rho_j}\right)_s = C_j^2 \qquad (j = 1, 2) \tag{3}$$

where the subscript s represents an isentropic condition and C_j is the velocity of sound in the gas medium.

The flowfield solutions to the preceding governing equations must satisfy the following kinematic and dynamic boundary conditions at the two liquid–gas interfaces, $y \approx \pm a + \eta_\pm$,

$$v_j = \left(\frac{\partial}{\partial t} + U_j^*\frac{\partial}{\partial x}\right)\eta_\pm \qquad (j = \ell, 1, \text{ and } 2) \tag{4}$$

$$\mu_\ell\left(\frac{\partial u_\ell}{\partial y} + \frac{\partial v_\ell}{\partial x}\right) = 0 \tag{5}$$

$$p_\ell - p_j - 2\mu_\ell\frac{\partial v_\ell}{\partial y} \pm \sigma\frac{\partial^2\eta_\pm}{\partial x^2} = 0 \qquad (j = 1 \text{ and } 2) \tag{6}$$

where μ_ℓ is the dynamic viscosity of the liquid, σ is the surface tension, η_+ and η_- are the interfacial displacements from the unperturbed position $y = +a$ and $-a$, respectively, and the plus sign before the surface tension σ is associated with the interface $y = +a$ and the minus sign with $y = -a$.

Solutions representing unstable wave motion are sought in terms of the following normal mode:

$$(\boldsymbol{u}_j, p_j, \rho_j, \eta_+, \eta_-) = [\tilde{\boldsymbol{u}}_j(y), \tilde{p}_j(y), \tilde{\rho}_j(y), \eta_{0,+}, \eta_{0,-}]\exp(\omega t + ikx) \tag{7}$$

Then the bounded solution for the disturbance-induced flowfield is obtained by the substitution of the preceding equation into the governing equations [Eqs. (1–3)] with a set of integration constants, which can be determined by the boundary conditions [Eqs. (4–6)]. Finally, the requirement of nontrivial solution results in the following dispersion relation governing the characteristics of the unstable wave motion and the ratio of initial disturbance amplitude at the two gas–liquid interfaces:

$$L_v L_s + \tfrac{1}{2}\left[r_1(\Omega + imU_1)^2 - r_2(\Omega + imU_2)^2\right](L_v + L_s) = 0 \tag{8}$$

$$\eta_{0,-}/\eta_{0,+} = (L_v - L_s)/(L_v + L_s) \tag{9}$$

where

$$L_s = \left\{[(\Omega + im) + 2m^2/Re]^2\tanh(m) - (4m^3/Re^2)S\tanh(S) + r_2(\Omega + imU_2)^2 + m^3/We\right\} \tag{10}$$

$$L_v = \left\{[(\Omega + im) + 2m^2/Re]^2\coth(m) - (4m^3/Re^2)S\coth(S) + r_2(\Omega + imU_2)^2 + m^3/We\right\} \tag{11}$$

and the other dimensionless parameters are as follows: Ω, the complex eigenfrequency; m, the disturbance wave number; Re; We; U_j; and d_j. This choice for the Mach number is based on experimental observations[22,23] that waves form on the liquid–gas interfaces and then propagate from the wavy liquid sheet surfaces into the compressible gas stream.

Comparison of the present results [Eqs. (8) and (9)] with those of the liquid sheet in incompressible gas stream of Li[7] indicates that the gas-phase compressibility effect enters the dispersion relation through the gas-phase pressure fluctuations via the normal stress boundary condition. That is, the effect of gas stream compressibility effectively modifies the gas-to-liquid density ratios according to the expression r_j given earlier. Further analysis and numerical computation show that the denominater in the r_j expression is smaller than one, thus the gas-phase compressibility essentially increases the gas-to-liquid density ratio d_j. Because it is generally known that increasing the density ratio d_j enhances the degree of sheet instability,[7] gas compressibility will promote the instability and breakup of the liquid sheets. It is also evident that the present results for the dispersion relation [Eq. (8)] and the initial disturbance amplitude ratio [Eq. (9)] reduce to those of the incompressible case investigated by Li[7] when the Mach number M_j vanishes.

From Eqs. (8) and (9), it becomes clear that when $\bar{\rho}_1 = \bar{\rho}_2$ and $U_1 = U_2$, we have either $L_s = 0$ and $\eta_{0,-}/\eta_{0,+} = +1$ or $L_v = 0$ and $\eta_{0,-}/\eta_{0,+} = -1$. The former corresponds to the two interfacial waves having a zero phase angle difference θ as shown in Fig. 1, which is often called sinuous mode of disturbances, and the latter corresponds to the two interfaces being displaced out of phase, which is usually referred to as the varicose mode. In general, the two interfaces will be displaced neither exactly in phase nor out of phase; however, one of the two unstable solutions closely resembles the sinuous mode. Hence, it will be called the parasinuous mode and the other solution the paravaricose mode. Note that only r_2 appears in Eqs. (10) and (11) because $L_s = 0$ and $L_v = 0$ would be the dispersion relation for the sinuous and varicose mode, respectively, if the flow conditions for the two gas streams are the same, that is, $d_1 = d_2$ and $U_1 = U_2$, hence, $r_1 = r_2$. The different conditions in the two gas streams are reflected in the square bracket term in the dispersion relation [Eq. (8)].

To investigate the effect of gas compressibility on the liquid sheet instability, we will seek solutions to the dispersion relation [Eq. (8)] under various flow conditions. Because the spatial instability of plane liquid sheets is related to the temporal instability[9] through Gaster's transformation,[10] only temporal instability will be presented in this study. In the context of temporal analysis, the real part of the complex eigenfrequency $\Omega = \Omega_{\mathrm{Re}} + i\Omega_{\mathrm{Im}}$ is often called the growth rate, which represents the degree of the liquid sheet instability. Because the dispersion relation cannot be solved analytically in closed forms, a numerical procedure has been implemented through the use of Muller's method.[24] Numerical iteration is terminated when the relative error between the successive iterations for the eigenvalue Ω satisfies a preset tolerance, which is usually 10^{-4} or less in the present study.

Results and Discussion

Before we present the results concerning the characteristics of the instability, it will be useful to analyze the cutoff wave number for the two unstable modes. The cutoff wave number is the maximum wave number of unstable disturbances, and, hence, it can be determined by setting the real part of the eigenfrequency Ω_{Re} to zero in the dispersion relation [Eq. (8)]. After some algebraic manipulations, it is found that there exist two cutoff wave numbers given here:

$$m_{0,1} = \frac{d_1 We(1-U_1)^2}{\left\{1 - M_1^2(1-U_1)^2\right\}^{\frac{1}{2}}} \tag{12}$$

$$m_{0,2} = \frac{d_2 We(1-U_2)^2}{\left\{1 - M_2^2(1-U_2)^2\right\}^{\frac{1}{2}}} \tag{13}$$

Clearly, the range of the unstable wave numbers depends on the Weber number, gas-to-liquid density ratio, gas velocity, and gas compressibility, but is independent of the liquid viscous effect. Viscosity certainly affects the disturbance growth rate and the maximum mode of instability, but it does not change the cutoff wave number. This result is consistent with earlier studies.[6,7]

Also note that the cutoff wave number given in Eq. (12) is clearly related to the upper gas–liquid interface, is influenced by the flow conditions across that interface, and is completely independent of the flow conditions of the other gas stream, that is, the lower one, that is not adjacent to that interface. Similar behavior is observed for the other cutoff wave number shown in Eq. (13). However, numerical computation indicates that the growth rate is dependent on the flow conditions of not only the liquid sheet, but also of both of the gas streams. Furthermore, the parasinuous mode is always associated with the larger of the two cutoff wave numbers and the paravaricose mode with the smaller cutoff wave number. Therefore, the cutoff wave number is equal to $\max(m_{0,1}, m_{0,2})$ for the parasinuous mode and $\min(m_{0,1}, m_{0,2})$ for the paravaricose mode. Physically, it implies that the parasinuous mode is related to the larger of the two relative velocities between the liquid and gas streams and the paravaricose mode to the smaller relative velocity. Hence, the growth rate for the parasinuous mode is usually larger than its counterpart for the paravaricose mode, and the former typically is dominant in practice. These observations are almost the same as for the incompressible case studied by Li.[7]

Furthermore, Eqs. (12) and (13) can be expressed in terms of a Weber number defined by $\rho_\ell (U_\ell^* - U_j^*)^2 a/\sigma$ and a Mach number defined by $(U_\ell^* - U_j^*)/C_j$. Hence, it reveals that both cutoff wave numbers depend on the relative velocities between the liquid and gas streams and that they are independent of the absolute liquid and gas velocities. However, as will be shown later, numerical calculations indicate that the growth rates are a function of the absolute velocities for the parasinuous mode at small liquid Weber numbers, of the relative velocities for the parasinuous mode at large Weber numbers, and for the paravaricose mode at any Weber numbers. These results are identical to the results of Li's previous study.[7]

Figure 2 shows the effect of gas compressibility on the cutoff wave number for the conditions of $We = 10^3$ and $d_j = 10^{-3}$, where j can be either 1 or 2. It is clear that the cutoff wave number $m_{0,j}$ increases slowly with the Mach number until M_j reaches a critical value. Then $m_{0,j}$ increases significantly and approaches infinity at the critical Mach number $M_j = |1/(1-U_j)|$, which corresponds to the vanishing of the denominator in Eqs. (12) and (13). Therefore, the gas compressibility effect will be felt with much smaller Mach numbers at high gas velocities as compared with the cases at low gas velocities. It should also be pointed out that Chawla[25] has shown that, for the unity Mach number, the cutoff wave number for the instability of a gas–liquid interface is always infinitely large for an

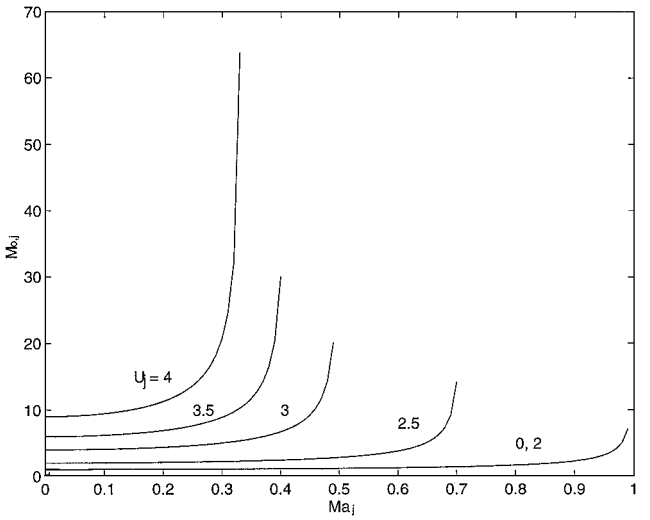

Fig. 2 Cutoff wave number as a function of the Mach number M_j and the dimensionless gas velocity U_j; $We = 10^3$ and $d_j = 10^{-3}$ (j can be either 1 or 2).

interface separating a moving gas and a stationary liquid stream. This corresponds to a unity dimensionless relative velocity across the interface when normalized by the moving stream velocity; thus, the critical Mach number reduces to one according to the present result.

Figure 3 presents the dimensionless wave growth rate Ω_{Re} as a function of the wave number for both parasinuous and paravaricose modes of disturbances for the flow conditions of $We = 10^3$, $Re = 10^3$, $d_1 = d_2 = 10^{-3}$, $U_2 = 0$, and $U_1 = 2$. It is seen that the growth rate and dominant and cutoff wave numbers all increase significantly with the Mach number, which indicates that the gas compressibility enhances the liquid sheet instability and promotes the liquid sheet breakup processes. It is also clear that the growth rate for the parasinuous mode is much larger than that for the corresponding paravaricose mode under the same flow conditions. This suggests that the parasinuous mode of disturbances is more unstable and will predominate the liquid sheet breakup processes. Hence, it is the one observed in reality. This is because the parasinuous mode is always associated with the larger relative velocities between the liquid sheet and the gas stream, as discussed earlier. The results shown in Fig. 3 are representative of large Weber numbers.

Results typical for small Weber numbers are shown in Fig. 4, where the growth rates for the parasinuous mode are computed for the flow conditions of $We = 3$, $Re = 10^2$, $d_1 = d_2 = 0.1$, $U_2 = 0$, and $U_1 = 1$. Clearly, the growth rate curves are quite different from those at large Weber numbers. Specifically, the growth rate curves exhibit two local maxima. The first peak at the smaller wave numbers, which has been referred to as the aerodynamic instability by Li and Tankin[6]

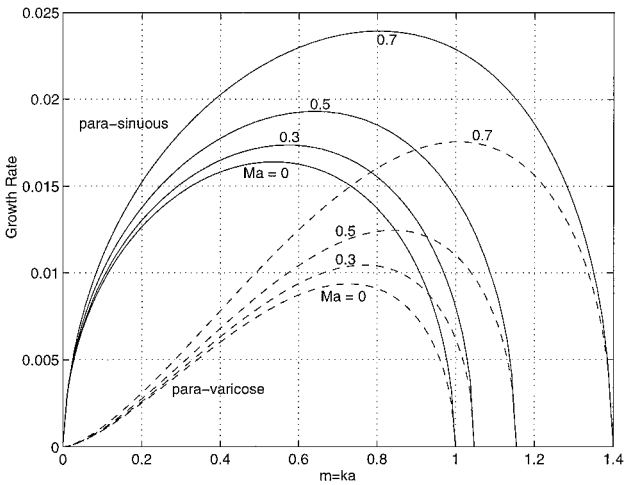

Fig. 3 Dimensionless wave growth rate for parasinuous and paravaricose modes; $We = 10^3$, $Re = 10^3$, $d_1 = d_2 = 10^{-3}$, $U_2 = 0$, $U_1 = 2$, and M ($= M_1 = M_2$) as shown.

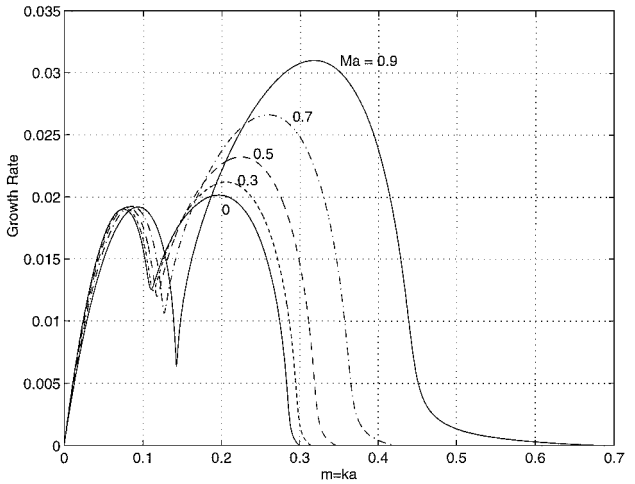

Fig. 4 Dimensionless wave growth rate for parasinuous mode; $We = 3$, $Re = 10^2$, $d_1 = d_2 = 0.1$, $U_2 = 0$, $U_1 = 1$, and M ($= M_1 = M_2$) as shown.

for the case of $M = 0$, increases only slightly with the Mach number, whereas the second peak at relatively large wave numbers, which has been called viscosity-enhanced instability by Li and Tankin,[6] increases significantly with the Mach number along with considerable increases in the dominant and cutoff wavenumbers. Again, this indicates the destabilizing effect of gas compressibility on liquid sheets.

The formation of two-peak growth rate curves is shown in Fig. 5 as a function of the gas velocity U_1 for the conditions of $We = 3$, $Re = 10$, $d_1 = d_2 = 0.1$, $U_2 = 0$, and $M_1 = M_2 = 0$. The zero values of the Mach numbers here represent the case of incompressible gas streams. Under these conditions, the growth rate only has one local maximum, corresponding to the aerodynamic instability described by Li and Tankin,[6] when the gas velocity $U_1 = 0$. As the gas velocity U_1 is increased gradually, the first peak decreases, and the second peak increases. The first peak becomes the smallest, and even smaller than the second peak, at $U_1 = 0.6$. As the gas velocity is increased further, both peaks increase. However, the first peak increases much faster than the second one, such that at $U_1 = 1.4$ the first peak dominates completely and the second peak disappears. It is evident that the second peak, whose presence is due to liquid viscosity,[6] can be promoted or suppressed by suitable values of gas velocities. Figure 5 also reveals that the growth rate values are different at the same relative velocity but different absolute velocities, for example, compare the growth rate at $U_1 = 0.6$, and 1.4 and 0 and 2. This demonstrates that the liquid sheet instability and breakup are controlled by the absolute, rather than relative, velocities at low Weber numbers. This result contrasts sharply with the case of large Weber numbers where the relative velocities are always predominant in influencing the instability characteristics.[7] Figure 6 shows the three-dimensional view of the two-peak formation in the growth

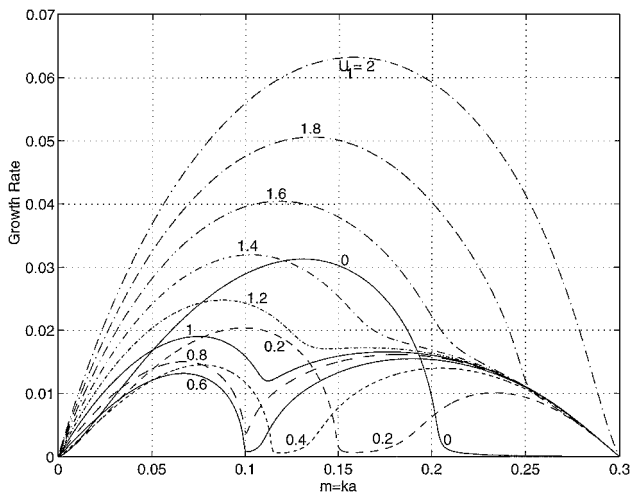

Fig. 5 Formation of two-peak wave growth rate for parasinuous mode; $We = 3$, $Re = 10$, $d_1 = d_2 = 0.1$, $U_2 = 0$, $M_1 = M_2 = 0$, and U_1 as shown.

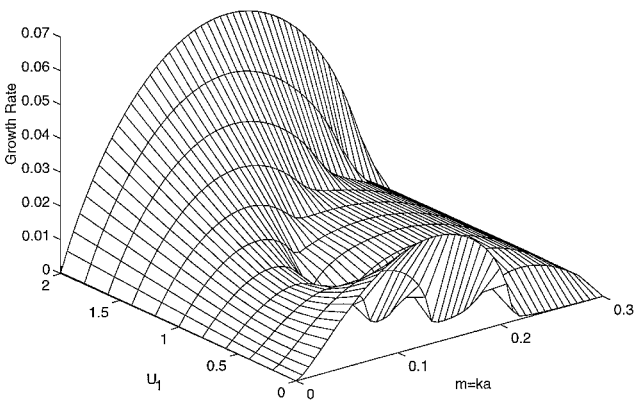

Fig. 6 Three-dimensional view of the two-peak formation in the growth rate of parasinuous mode; $We = 3$, $Re = 10$, $d_1 = d_2 = 0.1$, $U_2 = 0$, and $M_1 = M_2 = 0$.

rate curves. It is clear that a local minimum occurs at the wave number of around 0.1 and the gas velocity U_1 of around 0.5.

In practice, liquid sheet breakup is usually considered to be dictated by the maximum wave growth rate under a given set of flow conditions, and breakup occurs at the corresponding wave number, called the dominant wave number, which determines the sizes of subsequently formed droplets. Figures 7 and 8 show the variation of the maximum wave growth rate and the dominant wave number, respectively, for various Weber numbers as a function of the Mach number M $(=M_1=M_2)$ for both parasinuous and paravaricose modes under the conditions of $Re=10^5$, $d_1=d_2=10^{-3}$, $U_2=0$, and $U_1=2$, where the solid curves represent the results for the paravaricose mode and dashed curves the parasinuous mode. It is seen that both the maximum growth rate and the dominant wave number increase with both Weber and Mach numbers, and the increase becomes more pronounced and considerable at large values of Weber number and Mach number. Hence, liquid sheet atomization will be enhanced by the gas compressibility effects. It is also shown that the parasinuous mode has larger growth rate than the corresponding paravaricose mode, signifying its dominance over the liquid sheet instability processes, as discussed earlier. However, the dominant wave number for the paravaricose mode is larger than that for the parasinuous mode.

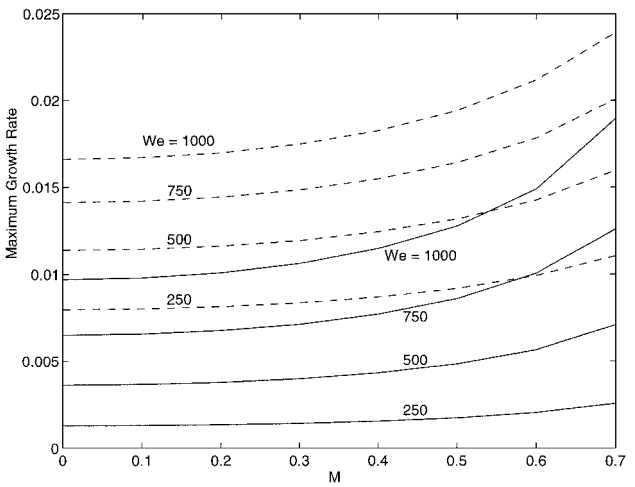

Fig. 7 Maximum wave growth rate as a function of the Mach number M $(=M_1=M_2)$ for both parasinuous and paravaricose mode; $Re=10^5$, $d_1=d_2=10^{-3}$, $U_2=0$, $U_1=2$, and *We* as shown: ——, paravaricose mode, and – – –, parasinuous mode.

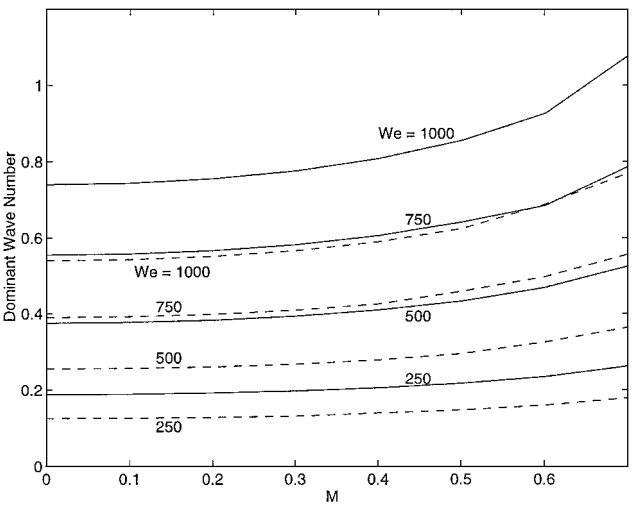

Fig. 8 Dominant wave number as a function of the Mach number M $(=M_1=M_2)$ for both parasinuous and paravaricose mode; $Re=10^5$, $d_1=d_2=10^{-3}$, $U_2=0$, $U_1=2$, and *We* as shown: ——, paravaricose mode, and – – –, parasinuous mode.

Conclusions

This paper reports a linear stability analysis of viscous incompressible liquid sheets in two compressible gas streams of unequal velocities. The results show that there exist two independent unstable modes: parasinuous and paravaricose. Although both modes are unstable, the parasinuous mode is predominant under the conditions typically found for practical applications of liquid atomization and sprays. Gas compressibility increases the wave growth rate and dominant wave number for both of the unstable modes; hence, it can enhance significantly the breakup of liquid sheets and the production of small droplets in sprays.

References

[1]Masters, K., *Spray Drying Handbook*, 4th ed., Wiley, New York, 1985, Chap. 1.

[2]Lefebvre, A. H., *Gas Turbine Combustion*, McGraw–Hill, New York, 1983, pp. 14, 15.

[3]Lefebvre, A. H., *Atomization and Sprays*, Hemisphere, New York, 1989, p. 7.

[4]Squire, H. B., "Investigation of the Instability of a Moving Liquid Film," *British Journal of Applied Physics*, Vol. 4, June 1953, pp. 167–169.

[5]Hagerty, W. W., and Shea, J. F., "A Study of the Stability of Plane Fluid Sheets," *Journal of Applied Mechanics*, Vol. 22, Dec. 1955, pp. 509–514.

[6]Li, X., and Tankin, R. S., "On the Temporal Instability of a Two-Dimensional Viscous Liquid Sheet," *Journal of Fluid Mechanics*, Vol. 226, May 1991, pp. 425–443.

[7]Li, X., "On the Instability of Plane Liquid Sheets in Two Gas Streams of Unequal Velocities," *Acta Mechanica*, Vol. 106, Nos. 1–4, 1994, pp. 137–156.

[8]Lin, S. P., Lian, Z. W., and Creighton, B. J., "Absolute and Convective Instability of a Liquid Sheet," *Journal of Fluid Mechanics*, Vol. 220, Nov. 1990, pp. 673–689.

[9]Li, X., "Spatial Instability of Plane Liquid Sheets," *Chemical Engineering Science*, Vol. 48, No. 16, 1993, pp. 2973–2981.

[10]Gaster, M., "A Note on the Relation Between Temporally-Increasing and Spatially-Increasing Disturbances in Hydrodynamic Stability," *Journal of Fluid Mechanics*, Vol. 14, Pt. 2, 1962, pp. 222–224.

[11]Li, X., "Spatial Instability of Plane Liquid Sheets," *Mixed-Flow Hydrodynamics*, edited by N. P. Cheremisinoff, Advances in Engineering Fluid Mechanics Series, Gulf, Houston, TX, 1996, Chap. 7, pp. 145–166.

[12]Li, H. S., and Kelly, R. E., "The Instability of a Liquid Jet in a Compressible Airstream," *Physics of Fluids A*, Vol. 4, No. 10, 1992, pp. 2162–2168.

[13]Zhou, Z. W., and Lin, S. P., "Effects of Compressibility on the Atomization of Liquid Jets," *Journal of Propulsion and Power*, Vol. 8, No. 4, 1992, pp. 736–740.

[14]Zhou, Z. W., and Lin, S. P., "Absolute and Convective Instability of a Compressible Jet," *Physics of Fluids A*, Vol. 4, No. 2, 1992, pp. 277–282.

[15]Lian, Z. W., and Reitz, R. D., "The Effect of Vaporization and Gas Compressibility on Liquid Jet Atomization," *Atomization and Sprays*, Vol. 3, No. 2, 1993, pp. 249–264.

[16]Chen, T., and Li, X., "Liquid Jet Atomization in a Compressible Gas Stream," *Journal of Propulsion and Power*, Vol. 15, No. 3, 1999, pp. 369–376.

[17]Mansour, A., and Chigier, N., "Disintegration of Liquid Sheets," *Physics of Fluids A*, Vol. 2, No. 5, 1990, pp. 706–719.

[18]Hashimoto, H., and Suzuki, T., "Experimental and Theoretical Study of Fine Interfacial Waves on Thin Liquid Sheet," *JSME International Journal*, Series II, Vol. 34, No. 2, 1991, pp. 277–283.

[19]Drazin, P. G., and Reid, W. H., *Hydrodynamic Stability*, Cambridge Univ. Press, New York, 1981, p. 155.

[20]Lin, S. P., and Ibrahim, E. A., "Stability of a Viscous Liquid Jet Surrounded by a Viscous Gas in a Vertical Pipe," *Journal of Fluid Mechanics*, Vol. 218, Sept. 1990, pp. 641–658.

[21]Lin, S. P., and Lian, Z. W., "Mechanisms of the Breakup of Liquid Jets," *AIAA Journal*, Vol. 28, No. 1, 1990, pp. 120–126.

[22]Sherman, A., and Schetz, J. A., "Breakup of Liquid Sheets and Jets in a Supersonic Gas Stream," *AIAA Journal*, Vol. 9, No. 4, 1971, pp. 666–673.

[23]Schetz, J. A., Kush, E. A., and Joshi, P. B., "Wave Phenomena in Liquid Jet Breakup in a Supersonic Crossflow," *AIAA Journal*, Vol. 18, No. 7, 1980, pp. 774–778.

[24]Muller, D. E., "A Method for Solving Algebraic Equations Using an Automatic Computer," *Mathematical Tables and Other Aids to Computation*, Vol. 10, No. 5, 1956, pp. 208–215.

[25]Chawla, T. C., "The Kelvin–Helmholtz Instability of the Gas–Liquid Interface of a Sonic Gas Jet Submerged in a Liquid," *Journal of Fluid Mechanics*, Vol. 67, Pt. 3, 1975, pp. 513–537.